doi: 10.5028/jatm.2012.04014711

Indoor Radar Cross Section Measurements of Simple Targets

Marcelo Alexandre Souza Miacci[1], Evandro Luís Nohara[2], Inácio Malmonge Martin[2], Guilherme Gomes Peixoto[3], Mirabel Cerqueira Rezende[3,*]

[1]Instituto Tecnológico de Aeronáutica - São José dos Campos/SP - Brazil

[2]Universidade de Taubaté - Taubaté/SP - Brazil

[3]Instituto de Aeronáutica e Espaço - São José dos Campos/SP - Brazil

Abstract: *This paper has described the radar absorbing materials characterization and radar cross section measurements, in the frequency range of 8 to 12 GHz, using a very simple setup. Simple targets like sphere, cylinder, flat plate, and dihedral corner were characterized by measuring the backscattered radiation patterns when these targets were illuminated by monostatic microwave radiation. Measurements were carried out inside an anechoic chamber (9x5x4m^3). Typical radar cross section patterns were obtained in different aspect angles, by rotating the targets around their vertical axes. The measured values and the theoretical previsions for each metallic target showed that the used setup guarantees a good precision of the obtained data. By recovering one of the targets, a cylinder, with a specific radar absorbing material developed at Materials Division of the Brazilian Aeronautics and Space Institute, it was possible to compare the obtained patterns and to discuss the influence of radar absorbing materials on the observed radar cross section reduction patterns. The used methodology showed to be useful for attending aeronautical and telecommunication applications.*

Keywords: *Radar Cross Section, Radar Absorbing Materials, Microwave Measurements.*

INTRODUCTION

Radar cross section (RCS) is the equivalent effective area of a target when it is impinged by a radar wave. In other words, the RCS measures the target ability to reflect radar signals impinged on it into the radar receiver. Radio Detection and Ranging (Radar) systems were developed in the 1940's, mainly to attend military purposes (Skolnik, 1990). Radar is an active remote system that has its own source of energy to produce images. Thus, it does not require sunlight as the optical systems, and data can be acquired either by day or by night. Furthermore, due to the specific wavelength of radar (microwave spectrum), cloud cover or smog can be penetrating by this radiation without any effect on the imagery.

Radar is based on the transmission and reception of pulses in a narrow beam. In this paper, this frequency range involved centimeter length of the electromagnetic spectrum. The returning echoes were then recorded, taking into consideration their power, time interval, and wave phases. The received power by the antenna from the transmitted radar pulse was directly connected with the physical characteristics of the target through the backscattering coefficient. The value of this backscattering coefficient is basically dependent on three factors: the target surface roughness; the target material composition (electrical and/or magnetic properties), and the wavelength of the radar.

The RCS of a target can be viewed as a comparison of the reflected signal power from it to the reflected one from a perfectly smooth sphere with a cross section area of 1m^2. The conceptual definition of RCS includes the fact that only one part of the radiated energy reaches the target. The RCS of a target (σ) is most easily visualized as the product of three parameters (Knott *et al*.,1993).

σ = Projected cross section x reflectivity x directivity.

The RCS (σ) is used in the range radar equation representing exactly the re-radiated (scattered) power from the target (Eq. 1), that is (Hartman and Berlekamp, 1988; Knott *et al*.,1993):

$$R^4 = \frac{Pt}{Pr}\frac{G^2\lambda^2}{(4\pi)^3}\sigma \quad (1)$$

Received: 07/10/11. Accepted: 22/11/11

*author for correspondence: mirabelmcr@iae.cta.br /Pç. Mal. Eduardo Gomes, 50. CEP: 12.228-901 - São José dos Campos/SP - Brazil

where,
R: distance between radar and target (m);
Pt: radar transmitted power (W);
Pr: radar received power (W);
G: antenna gain;
λ: wavelength (m).

The reflectivity is defined as the intercepted radiated (scattered) power by the target. The directivity is given by the ratio of the backscattered power into the direction of the radar to the power, which would have been backscattered, considering a uniform scattering in all directions (isotropic). The sphere is the unique target that the RCS is independent of the frequency if operating at sufficiently high frequency, where λ<<range, and also λ<<target radius (*R*). Experimentally, the radar return reflected from a target is compared to the one reflected from a sphere, which has a frontal or projected area of one square meter, i.e., a diameter of 1.13m (Knott *et al*.,1993). In general, the RCS of a sphere is taken as a reference value. If calibrated, other targets like cylinders, flat plates, corner reflectors, and Luneberg lens can also be used for comparative RCS measurements.

Considering the RCS reduction, these targets can be recovered using layers of radar absorbing materials (RAM). They can be classified in two broad categories, dielectric and magnetic absorbers (Rezende *et al.*,2003; Johnson, 1992; Lee, 1991). Dielectric absorbers depend on the ohmic loss of the energy that can be achieved by loading lossy fillers, such as carbon black, graphite, conducting polymers, and metallic particles (Faez *et al*., 2000; Faez *et al*., 2005; Folgueras *et al*., 2007; Biscaro *et al.,* 2008; Folgueiras *et al*., 2010). The molecules in this kind of lossy material are essentially small dipoles that try to orient themselves along the incident field. If the field changes too fast or if the dipoles lag the impressed field variations, the material absorbs the incident radiation (Knott et al.,1993). Magnetic absorbers depend on magnetic losses, which are obtained when magnetic particles like ferrites and carbonyl iron are filled into a polymeric matrix (Gama and Rezende, 2010; Gama *et al*.,2011; Silva *et al*., 2009).

Figure 1 shows the calculated RCS values of simple targets commonly employed in experimental measurements.

The RCS measurements can be carried out using different techniques, depending on the shape of the target. When RAM efficiency is evaluated by RCS measurements is common to use a double face panel, where one side is used as a reflector material (reference), and the other is coated with RAM. The panel is fixed on a rotating support, which is positioned in front of the receiving and transmitting horns. The advantage of this methodology is that it allows the evaluation of the reference and the absorbing material by rotating the device from 0 to 360º, characterizing both sides of the panel, one after the other. Figure 2 depicts a simplified scheme of a common device used in the RCS technique (Currie, 1989; Miacci, 2002). The use of this device allows to characterize the reference and the RAM using the same experiment, because the RCS diagram

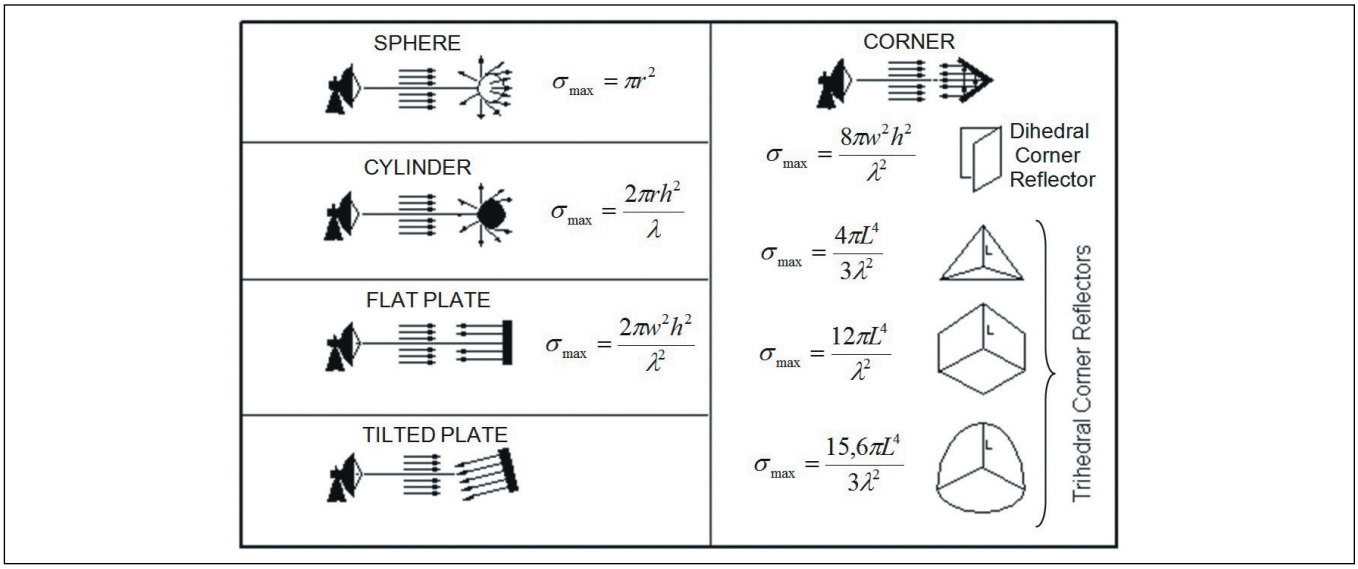

Figure 1. Backscattering from simple shapes (targets) and the RCS equations for each target. *r*: radius of sphere or cylinder; *h*: cylinder, flat plate or dihedral length; *w*: flat plate and dihedral width; *L*: trihedral length. Tilted Plate reflects away from the plate and could be zero reflected to radar. Based on Johnson, 1992.

of flat plat recovered with RAM is obtained by rotating the device from 0º to 180º and the reference (metal flat plate) is get from 180º to 360º . Thus, this methodology is considered a self-calibrating measurement, once the perpendicularity of the device is guaranteed (Currie, 1989; Miacci, 2002).

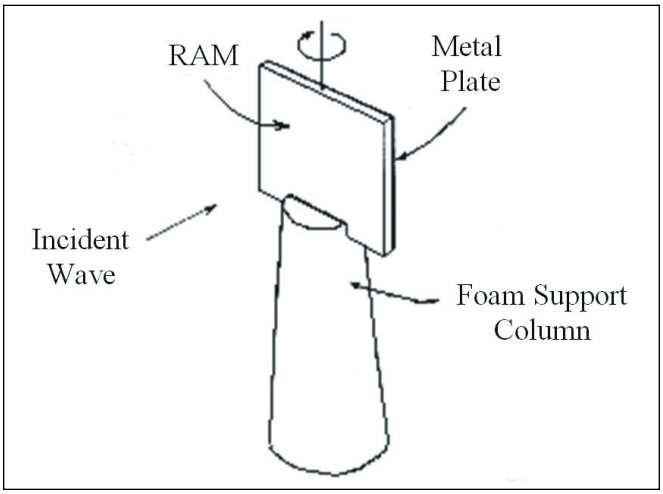

Figure 2. Device scheme used in the RCS method. Based on Miacci, 2002.

In order to have good precision, it is necessary to take care with the alignment between the transmitter/receiver antennas and the target (Burgess and Berlekamp, 1988). The use of a laser beam helps in the alignment of the system, improving the precision of the measurements. Figure 2 also shows the support column for the target, called pylon, which needs to be recovered with RAM in order to avoid any possible contribution of the reflective wave, which prejudices the target characterization.

Using this procedure for simple targets and placing the transmitter (TX) and receiver (RX) antennas in the scheme showed in Fig. 3, it is possible to measure the RCS in different frequency ranges. The distance between both antennas needs to be tested in order to eliminate the radiation coupling between them, in near space of the setup.

The RCS patterns depend exactly on the target object shape and also on the incidence angle of waves on the same object. The sphere pattern is essentially the same in all directions. The flat plate RCS is strongly dependent on its position in relation toward the radar. The corner reflector has a RCS pattern as high as the flat plate dimensions, with the maximum peaks in the angle range of +60º and -60º. The returned waves from a corner reflector seem analogous to the ones reflected by a flat plate, maintaining the perpendicularity to the line of the transmitter and receiver antennas.

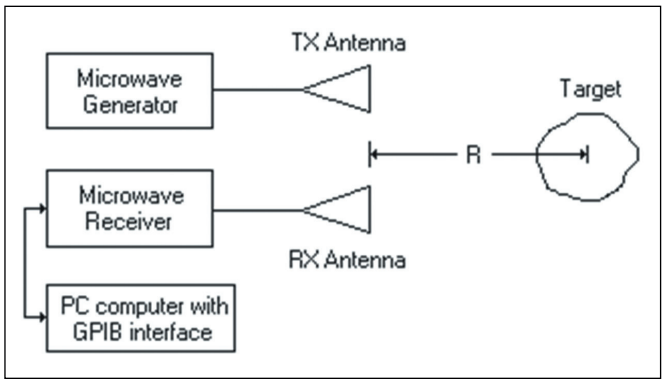

Figure 3. RCS measurement setup (*R* is the distance between the antennas and the target) (Miacci, 2002).

Targets such as ships and aircraft are composed with many effective simple targets as cylinder and corners. An aircraft is a very complex target in terms of RCS signature. It has many reflecting elements and shapes. The RCS of a real aircraft varies significantly depending upon the direction and the frequency band of the illuminating radar.

This work showed a study involving RCS measurements of simple targets (flat plate, cylinder, sphere, and dihedral), by using a simple setup projected and built in an anechoic chamber belonged to *Instituto de Fomento e Coordenação Industrial do Departamento de Ciência e Tecnologia Aeroespacial* (IFI/DCTA), in the frequency range of 8 to 12GHz. RCS reduction measurements were obtained by recovering the cylinder with a specific RAM processed at the Materials Division of *Instituto de Aeronáutica e Espaço* (IAE).

EXPERIMENTAL

The RCS measurements were carried out at the frequencies of 8, 9, 10, 11, and 12GHz. In each frequency, the target was fixed on the rotating support (Fig. 2) and rotated from 0 to 360º, at a scanning rate of 0.080rad/s. The built setup (Miacci *et al*., 2001a) for RCS measurements is constituted of: anechoic chamber, matched at 2 to 18GHz; sweep model HP 83630B (Hewlett Packard); spectrum analyzer model HP8593E; PC computer with HPIB interface; low loss coaxial cables from Huber-Suhner Company, model Sucoform SM-141-PE (50Ω); antennas in the range of 8 to 12GHz; Luneberg lens with RCS of 45m^2 at 9.375GHz, from Thomson CSF International Inc (Thomson, 1988); targets with different shapes - a flat plate with dimensions of (30x20)cm^2, a dihedral corner reflector with flat plates of (17x17)cm^2, a metallic cylinder of 32cm of high and 15cm of diameter, all in

aluminum 2024 T3, and a steel sphere of 60.96cm of diameter, and RAM coating developed at the Materials Division of the IAE.

The RAM preparation involved the mixture of 60% (weigh/weigh – w/w) of a commercial polyurethane matrix loaded with fillers, being NiZn ferrite (35% w/w) and carbon black (5% w/w). Physico-chemical characteristics of the fillers and the polyurethane resin as well as the coating preparation procedures were previously described (Dias, 2000). The RAM was applied on the target (cylinder) surface by brushing.

RESULTS AND DISCUSSION

Luneberg lens

In order to validate the proposed RCS measurement setup, firstly, a certified reference target called Luneberg lens of 30cm of diameter and RCS of 45m^2 was used. A Luneberg lens is a sphere constituted of dielectric massive shells. Figure 4 depicts a measured RCS diagram of this target using the built setup, in function of aspect angles between 0 and 180º, and frequency of 9.375GHz. The maximum power (Pmax=-35.0dBm) observed in this diagram corresponds to the RCS value of 45m^2, according to the certified value given by the manufacturer (Thomson, 1988). Using the relationship given by Eq. 2, it is possible to determine the RCS values of simple targets in the same frequency (9.375GHz). The constant intensity level of the signal (-35.0dBm), between the aspect angles of -65º and +65º, corresponds to the region with the same scattering level of the lens, being a characteristic RCS pattern for this target. The obtained RCS pattern shows good agreement with that one furnished by Thomson CSF International Inc, validating the built setup.

Using these data obtained with the Luneberg lens, it is possible to determine the RCS value for other simple targets based on Eq. 2 and given by Currie, 1989; Miacci *et al*., 2001b; Miacci *et al*., 2002:

$$\sigma_t = \frac{P_t}{P_r}\sigma_r \qquad (2)$$

where,
σt : RCS of the test target (m^2);
Pt: received power from test target (W);
Pr: received power from reference target (Luneberg lens) (W), and σr: RCS of the reference target (Luneberg lens) (m^2).

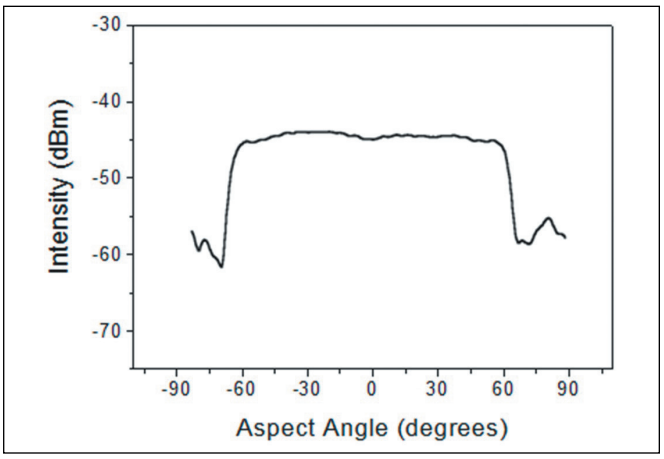

Figure 4. Measured RCS pattern of the Luneberg lens at 9.375GHz.

Dihedral

Figure 5 shows the plotted diagrams of the dihedral corner reflector at 9.375GHz. The theoretical RCS can be calculated using the expression given in Fig. 1. The typical diagram in Fig. 5 depicts three maximum value regions of RCS. Between -20º and +20º the value of -38.4dBm is due to the contribution of the interactions of reflected waves between the two plates. The second and third peaks at 45º and +45º, respectively, present an intensity of -41.3dBm, which is attributed to the individual contribution of each plate of the dihedral, separately. The calculated RCS value for this target at 9.375GHz is equal to 20.5m^2 and the experimental value is 20.6 m^2. The difference between these two RCS values is equal to 0.1 m^2 showing good agreement. Thus, the comparison of the RCS pattern of the Luneberg lens and the dihedral, both at 9.375GHz, allowed calibrating the dihedral in other frequencies.

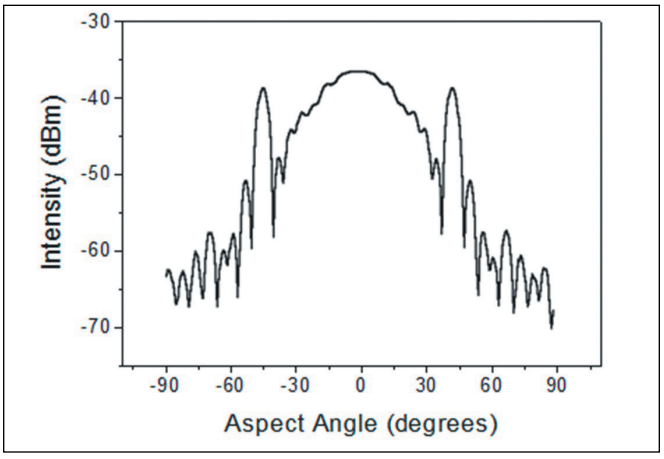

Figure 5. RCS diagram pattern of a dihedral corner reflector (17x17)cm^2 at 9.375GHz.

The RCS diagrams of the dihedral corner reflector in function of the frequency (from 8 to 12GHz) are shown in Fig. 6.

Figures 5 and 6 show that the RCS diagrams of the dihedral corner reflector target present nearly the same shapes in function of the frequency when the vertical axes rotates from -90º to +90º. Meanwhile, the amplitude (intensity in dBm) of the signals in the same aspect angles is slightly different with the frequency (Fig. 6).

Table 1 shows the measured and calculated RCS values for the dihedral at different frequencies. The determined deviation shows good agreement with the calculated values, using equations presented in Fig. 1, which confirm the adequate RCS methodology proposed.

Table 1. Theoretical and experimental measured RCS values of a dihedral of (17x17)cm^2 in function of the frequency.

Frequency (GHz)	Calculated RCS (m)	Measured RCS (m)
8.0	14.9	14.8
9.0	18.8	19.0
10.0	23.3	23.4
11.0	28.2	28.1
12.0	33.5	33.7

Metallic sphere

A metallic sphere with diameter of 60.96 cm was characterized at 8, 9, 10, 11, and 12GHz. Table 2 reports the measured and calculated RCS values for this sphere (using equation presented in Fig. 1). The mean value of determined RCS from the sphere was equal to 0.31 m^2, and the calculated value was 0.29 m^2. The small deviation between the measured and calculated values is is assigned to non-uniformity of the spherical surface of the target.

Table 2. RCS values of a metallic sphere (diameter of 60.96 cm) in function of the frequency.

Frequency (GHz)	Calculated RCS (m^2)	Measured RCS (m^2)
8.0	0.29	0.31
9.0	0.29	0.30
10.0	0.29	0.32
11.0	0.29	0.28
12.0	0.29	0.31

Flat plate

Figure 7 depicts a typical RCS diagram of an aluminum flat plate, at 8GHz, with a rotation of 180º. It is observed a peak at 0º corresponding to the value of -41.4dBm, attributed to the contribution of the normal incidence of the electromagnetic waves on the flat plate. The position (perpendicularity) of the plate is a very critical parameter for the success and precision of the measurements.

The RCS values of a perfect flat rectangular reflector can have its theoretical RCS value calculated as a function of the incident radiation frequency, according to equation depicted

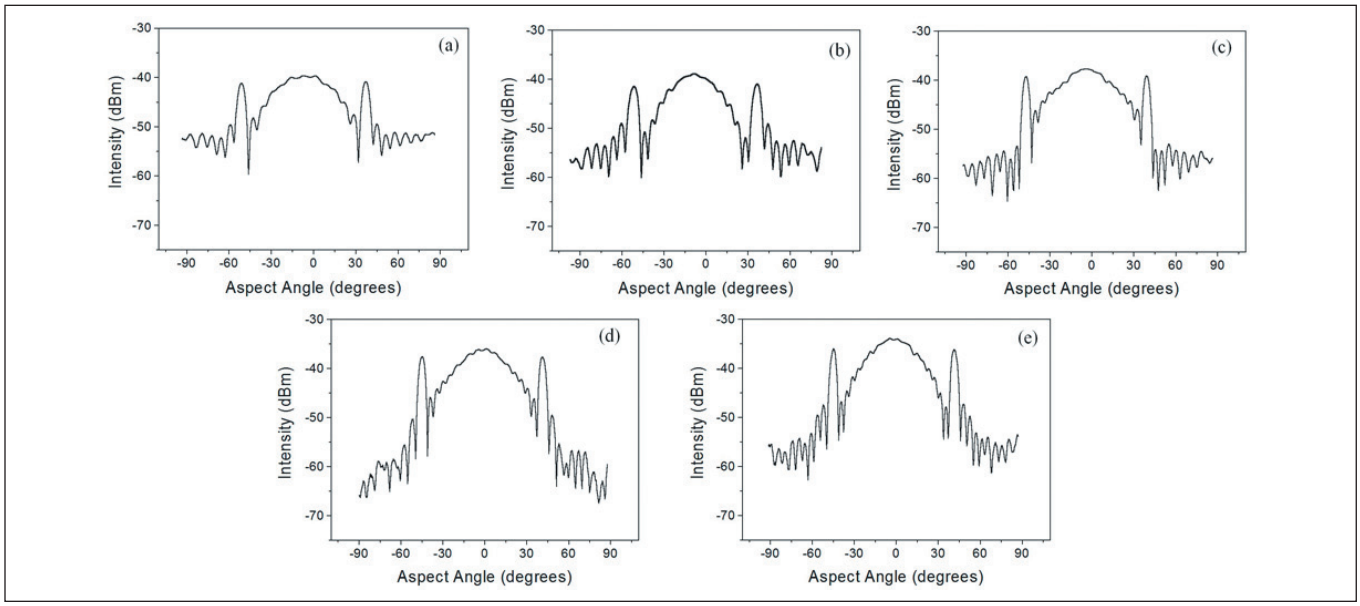

Figure 6. RCS patterns (dBm) of the dihedral of (17x17)cm^2, at: (a) 8.0GHz, (b) 9.0GHz, (c) 10.0GHz, (d) 11.0GHz, and (e) 12.0GHz.

in Fig. 1 (Johnson, 1992). Table 3 shows the calculated RCS values of an aluminum flat plate (20x17)cm², in function of frequency.

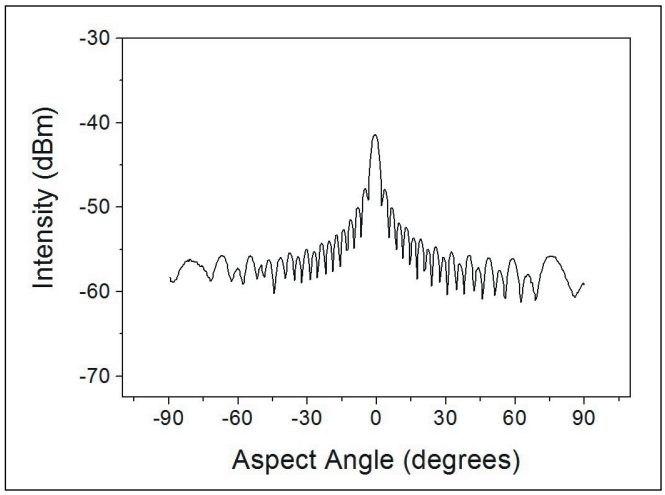

Figure 7. RCS diagram in dBm of an aluminum plate (20x17)cm² at 8GHz.

Figure 8 shows the equivalent RCS diagram of flat plate, in square meters, obtained at 8 GHz in function of the aspect angles of the incident wave. The measured peak, equal to –41.4dBm, at 8GHz (Fig. 7), was expressed in square meters (Fig. 8) and correlated with the calculated RCS value of 10.3m² (Table 3). This comparison shows good agreement confirming the proper adjustment of the used RCS setup.

Table 3. RCS values of a flat plate of (20x17)cm² in different frequencies.

Frequency (GHz)	Calculated RCS (m²)	Measured RCS (m²)
8.0	10.3	10.2
9.0	13.0	12.9
10.0	16.1	16.2
11.0	19.5	19.6
12.0	23.2	23.1

Metallic cylinder

Figure 9 depicts the plotted RCS diagram of a metallic cylinder of 32cm of length and 15cm of diameter, rotating the cylinder from +90º to -90º on its axes and keeping the TX and TR antennas in the same position, at 9.375GHz. The determined RCS value is constant and omnidirectional, equals to 1.61m². The cylinder RCS measurement need some tight adjusts on the dielectric support to avoid contributions of

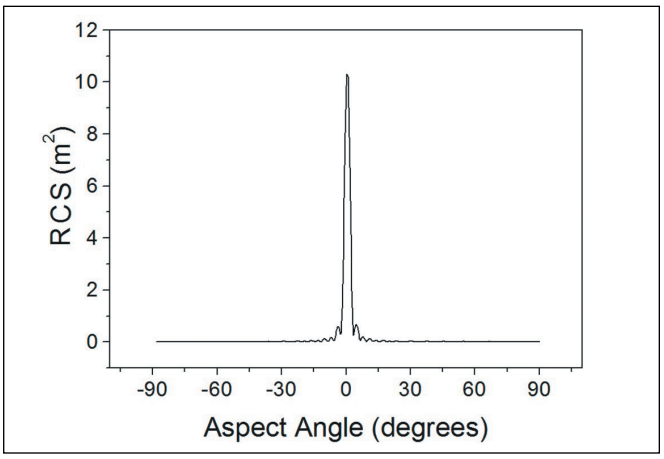

Figure 8. RCS diagram (m²) of an aluminum plate (20x17)cm² at 8GHz.

the reflected waves from this apparatus. The obtained RCS is almost constant at 9.375 GHz (-49.7±1.0dBm) rotating the support in 360º around its vertical axe. This curve is typical for this kind of target and it is attributed to the cylinder shape, which contributes only as a line when the wave impinges on it.

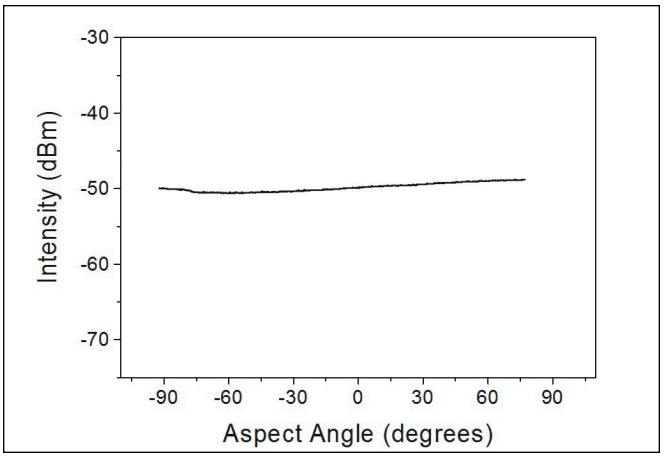

Figure 9. RCS diagram of a cylinder, at 9.375GHz

Afterwards, using the same RCS device and the same cylinder, it was obtained the RCS diagram of this target coated with a processed RAM. Figure 10 shows the RCS diagram of the cylinder coated with the RAM presenting 1.2±0.1mm of thickness loaded with NiZn ferrite and carbon black. In this case, the diagram shows the reflectivity variation in function of the aspect angles, characterizing a RCS reduction of the target. This variation is attributed to both the bulk heterogeneity of the processed RAM, related to the ferrite and carbon black particles distribution, and to the absorber thickness variation.

Using the curve (a) as reference, Fig. 10 shows that the absorbing propriety presents a reflectivity value of

-7.8dBm near –60º and a maximum value of -22.8dBm at +30º. Therefore, in these angles, the absorber presents more efficient attenuation values of the incident radiation. Figure 11 depicts the RCS diagram at 12GHz of the same cylinder coated with the RAM. In this case, the absorption mean value is lower than -7.8dBm (in relation to the values of curve (a)), showing that this material behaves as a more efficient absorber in higher frequency range. Again, it is observed that the used RAM reveals similar absorption behavior at 12GHz, showing better attenuation results near –60º and +30º aspect angles.

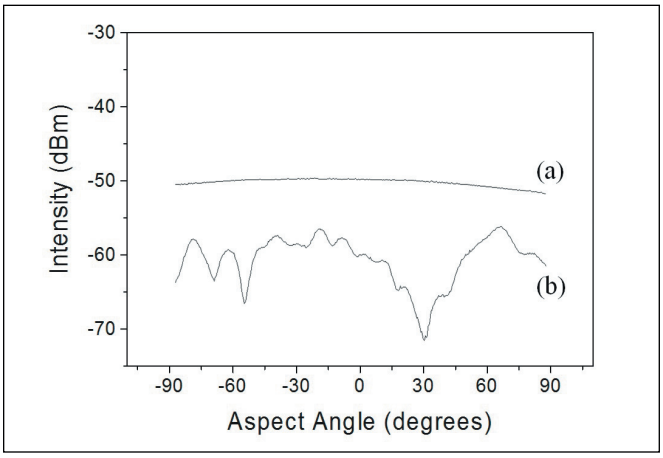

Figure 10. RCS diagrams of cylinder (a) without a RAM and (b) coated with a RAM, at 10GHz

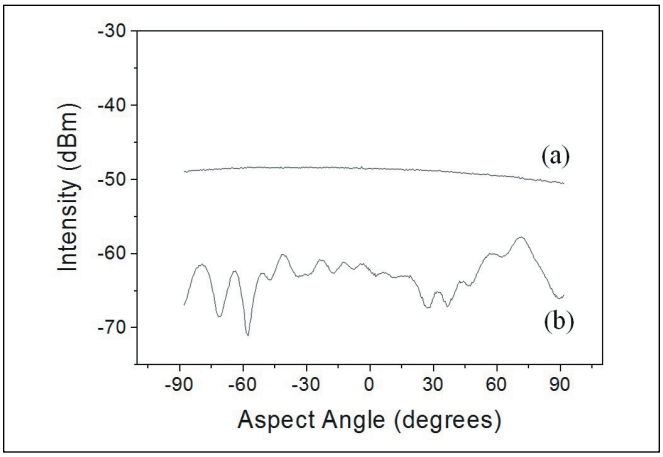

Figure 11. RCS diagrams of cylinder (a) without a RAM and (b) coated with a RAM, at 12GHz.

CONCLUSIONS

This paper presented a simple setup built inside an anechoic chamber (indoor measurements), proper to measure RCS of simple targets such as sphere, flat plates, Luneberg lens, dihedral corner reflectors, and cylinders. The validation of this setup was made by using a certified Luneberg lens with $45m^2$, which showed a very good agreement with the data furnished by the Luneberg lens manufacturer. Simple metallic targets, flat plates, cylinder, dihedral and sphere were characterized by measuring the backscattered radiation patterns in different aspect angles, in the frequency range of 8 to 12GHz. The comparison of the RCS data with that one calculated by theoretical equations showed good agreement. RCS reduction measurements were also made recovering a cylinder with RAM developed at the IAE. The obtained RCS patterns showed that this methodology is adequate to characterize this kind of material revealing that the used RAM reduced the RCS of the tested target and changed its reflectivity behavior as a function function of the aspect angles.

ACKNOWLEDGEMENTS

The authors thank *Fundação de Amparo à Pesquisa do Estado de São Paulo* (FAPESP) (project No. 98/15839-4), *Coordenação de Aperfeiçoamento de Pessoal de Nível Superior* (CAPES), *Conselho Nacional de Desenvolvimento Científico e Tecnológico* (CNPq) with projects 305478/2009-5 and 300228-87, and the *Estado-Maior da Aeronáutica* (EMAer) for the financial support.

REFERENCES

Biscaro, R.S. *et al*., 2008, “Influence of doped polyaniline on the interaction of PU/PAni blends and on its microwave absorption properties”, Polymers for Advanced Technologies, Vol. 19, pp 151-157.

Burgess, L. R. and Berlekamp, J., 1988, “Understanding Radar Cross-Section Measurements”, MSN & CT – Microwaves Systems News & Communications Technology, USA, pp. 54-61.

Currie, N.C., 1989, “Radar Reflectivity Measurement: Techniques and Applications”, 1st Edition, Artech House, Norwood, USA.

Dias, J. C., 2000, “Obtenção de Revestimentos Absorvedores de Radiação Eletromagnética (2-18) GHz Aplicados no

Setor Aeronáutico", PhD Thesis, Instituto Tecnológico de Aeronáutica, São José dos Campos, SP, Brazil.

Faez, R. *et al*., 2000, "Polímeros condutores intrínsecos e seu potencial em blindagem de radiações eletromagnéticas", Polímeros: Ciência e Tecnologia, Vol. 10, pp. 130-137.

Faez, R. *et al*., 2005, "Microwave Absorbing Coatings Based on a Blend of Nitrile Rubber, EPDM Rubber and Polyaniline", Polymer Bulletin (Berlin), Vol. 55, pp. 299-307.

Folgueras, L. C. *et al*., 2007, "Dielectric Microwave Absorbing Material Processed by Impregnation of Carbon Fiber Fabric with Polyaniline", Materials Research, Vol. 10, No. 1, pp. 95-99.

Folgueiras, L.C. *et al*., 2010, "Dielectric Properties of Microwave Absorbing Sheets Produced with Silicone and Polyaniline", Materials Research, Vol. 13, No. 2, pp. 197-201.

Gama, A.M. *et al*., 2010, "Complex permeability and permittivity variation of carbonyl iron rubber in the frequency range of 2 to 18 GHz", Journal of Aerospace Technology and Management, Vol. 2, pp. 59-62.

Gama, A.M. *et al*., 2011, "Dependence of microwave absorption properties on ferrite volume fraction in MnZn ferrite/rubber microwave absorbing materials", Journal of Magnetism and Magnetic Materials, Vol. 323, pp. 2782 - 2785.

Hartman, R. and Berlekamp, J., 1988, "Fundamentals of Antenna Test Evaluation". MSN & CT – Microwaves Systems News & Communications Technology, USA, pp. 8-20.

Johnson, R.N., 1992, "Radar Absorbing Material: A Passive Role in an Active Scenario", International Countermeasures Handbook, 11th Edition, E.W. Communications, Palo Alto, CA., USA.

Knott, E.F. *et al*., 1993, "Radar Cross Section". 2nd Edition, Artech House, Inc., Norwood, USA.

Lee, S. M., 1991, "International Encyclopedia of Composites", Vol. 6, VHC Publishers, New York, USA.

Miacci, M. A. S. *et al*., 2001a, "Método de Medida de Seção Reta Radar de Objetos Refletores de Ondas Eletromagnéticas na Faixa de 1 GHz a 100 GHz para Caracterização Eletromagnética de Materiais Absorvedores de Radiação Patente", Brazilian Patent (in analysis), MU8102042-2.

Miacci, M. A. S. *et al*., 2001b, "Radar Cross Section Measurements (8-12GHz) of Flat Plates Painted with Microwave Absorbing Materials", SBMO/IEEE, Belém, PA., Brazil, Vol. 1, pp. 263.

Miacci, M. A. S., 2002, MSc. Dissertation, "Determinação Experimental do Espalhamento Monoestático de Microondas por Alvos de Geometria Simples", Instituto Tecnológico de Aeronáutica, São José dos Campos, SP, Brazil.

Miacci, M. A. S. *et al*., 2002, "Medidas de Refletividade, Transparência e Seção Reta Radar (RCS) de Compósitos Avançados na Faixa de 8 – 12 GHz", Brazilian Microwave and Optoeletronics Symposium, Recife, Brazil.

Rezende, M.C. *et al*., 2003, "Reflectivity in the microwave range of polyurethane coating loaded with NiZn ferrites", Materials Research, Vol. 1, pp. 1-10.

Silva, V. A. *et al*., 2009, "Comportamento eletromagnético de materiais absorvedores de micro-ondas baseados em hexaferrita de Ca modificada com íons CoTi e dopada com La", Journal of Aerospace Technology and Management, Vol. 1, pp. 255-263.

Skolnik, M., 1990, "Radar Handbook", 2nd Edition, McGraw Hill, USA.

Thomson Inc., 1988, "Luneberg Reflectors and Lenses", Technical Bulletin, September, France.